Power Quality State Estimator for Smart Distribution Grids

A. Farzanehrafat, *Student Member, IEEE*, and Neville R. Watson, *Senior Member, IEEE*

***Abstract*—The importance of power quality issues, due to the significant losses for poor power quality, has resulted in research being focused on extending the concept of state estimation techniques into power quality issues. Under the umbrella of power quality state estimation (PQSE) as a smart algorithm, this paper focuses on one type, transient state estimation (TSE). The formulation of a new three-phase transient state estimator is given and its application to a realistic system demonstrated. The accuracy of the new transient state estimator is investigated by application to a test system to identify the cause of a voltage dip/sag in the presence of 5% measurement noise (normally distributed) in all the measurements.**

***Index Terms*—Power quality state estimation, smart algorithms, state estimation, transient state estimation.**

I. Introduction

THE need to modernize the grid to enable it to meet the needs of the future is well accepted [1], [2]. This has led to the Smart Grid concept as a pathway of increasing the smartness of the electrical grid so as to meet the demands of the future. Part of this involves advances in metering infrastructure which will make a large amount of data available in the future. Since advances in metering and deployment of advanced metering infrastructure (AMI) enables access to a wealth of data the issue is to turn the massive amount of data available into useful information that will help Smart Grids to evolve and achieve the desired functionalities. Smart algorithms are needed for the control of both generation and demand to improve management of the distribution system so as to maximize the efficiency, utilization, reliability and resilience of the infrastructure.

There is already a high level of smart algorithms already deployed in some electrical power systems, but these are specially schemes designed as one-off to overcome specifically identified problems. These are based on studying numerous contingencies and determining the best course of action. For example in New Zealand there are "run-back schemes". If a certain contingency occurs then generation in certain locations (or HVDC link) are backed-off to ensure remaining circuits are not overloaded, causing tripping. Run-back schemes are seen as a way of allowing new generation to connect while limiting or avoiding the need for asset upgrades [3]–[6].

Manuscript received December 07, 2011; revised March 21, 2012, June 18, 2012, August 12, 2012, and September 30, 2012; accepted October 27, 2012. Date of publication April 16, 2013; date of current version July 18, 2013. Paper no. TPWRS-01136-2011.

The authors are with the Electrical and Computer Engineering Department, University of Canterbury, Christchurch 8020, New Zealand (e-mail: ali.farzanehrafat@pg.canterbury.ac.nz; neville.watson@canterbury.ac.nz).

Color versions of one or more of the figures in this paper are available online at http://ieeexplore.ieee.org.

Digital Object Identifier 10.1109/TPWRS.2013.2254139

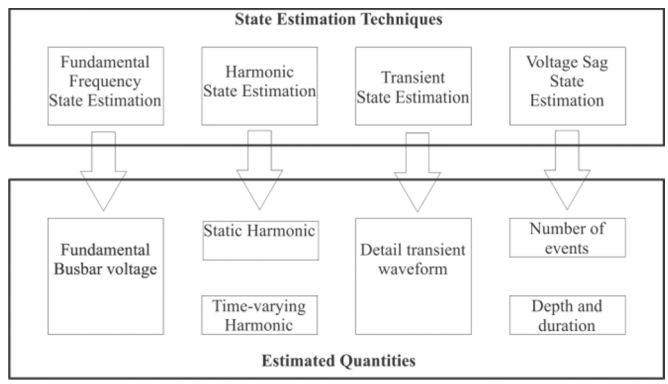

Fig. 1. Different type of PQSE.

Recently the importance of power quality issues and the reduction in price of meters capable of measuring power quality indices has resulted in research being focused on extending the concept of state estimation techniques into power quality issues. This area of research is called power quality state estimation (PQSE) [7], and represents a class of techniques as depicted in Fig. 1. Despite the different formulation and quantities they use, the common feature is that they are applying state estimation techniques to power quality problems. Harmonic state estimation (HSE) and identification of harmonic sources, transient state estimation (TSE) and voltage Dip/Sag state estimation (VDSE), are all types of PQSE. Therefore, PQSE is not one particular type of analysis but covers many different types in power quality area.

Proposing PQSE as a smart algorithm, this paper takes transient state estimation (TSE) further by formulating a new three-phase transient state estimator. An earlier contribution [7] introduced the concept of TSE using NIS on a single-phase system with lumped electrical circuit elements where the system is fully observable. This paper extends this to three-phase and demonstrates its applicability to unobservable systems.

This paper is organized as follows: Although an overview of the state-of-the-art techniques currently available for PQSE has been provided in [7] for completeness Section II reviews the concept of PQSE and the power quality phenomena. Section III describes how new transient state estimator is formulated and gives an overview of the implemented algorithm. Then, in Section IV, the implemented algorithm in MATLAB is applied to a distribution test system to investigate the accuracy of this approach to identify the cause a voltage dip/sag occurred in presence of 5% normally distributed noise in all the measurements. Finally, Section V draws conclusions from this work.

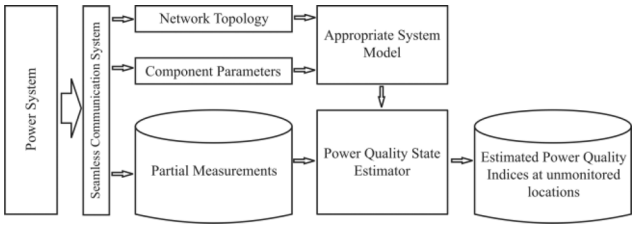

Fig. 2. Framework of PQSE.

II. Power Quality State Estimation

Power quality state estimation is a technique whereby the power quality at an unmonitored location can be estimated from limited number of measurements. Fig. 2 shows the framework of PQSE. Based on the network topology and component parameters, appropriate model of the system is formulated. Partial measurements provided by the seamless communication system are used as input for power quality state estimator unit to estimate the relevant power quality indices for unmonitored locations.

The exact way in which power quality is assessed and quantified depends on the particular issue and the potential problems [8], and this necessitates a different type of smart algorithm (PQSE) for each phenomena. Having identified some issue on the grid would then allow a smart algorithm to decide of the best course of action to minimize the disturbance to the grid. This may be given in terms of recommendations to the system operator or automated action. In fact, traditional fundamental frequency state estimation can be considered a PQSE as steady-state voltage (under- or over-voltage) is a power quality issue.

A. Harmonic State Estimation (HSE)

The task of HSE [9], [10] is to generate the "best" estimate of the harmonic levels from limited measured harmonic data, corrupted with measurement noise. This is the reverse of harmonic penetration in that the harmonic sources are unknown and the harmonic levels throughout the system is determined from a limited number of harmonic measurements.

A great deal of work has been done on HSE from different points of view such as finding the optimal number of the measurements and the best location of them [11], bad data analysis [12], varying harmonic levels with time [13], estimating the type of loads which generating harmonics [14]. Implementation of HSE, based on a field-test data in Japan also has been presented in [15].

B. Voltage Sag State Estimation (VSSE)

In the previous contributions, voltage sag state estimation (VSSE) is generally considered in two main areas. While first one refers to the number of voltage sags arising at unmonitored buses from the number (frequency) of sags obtained at a limited number of monitored buses, the second one refers to the use of estimation techniques to measure the sag level (magnitude) at every node of a distribution feeder.

In [16] a voltage sag state estimation method is proposed based on the fault positions concept calculates the residual voltage caused by faults occurring along lines. An integer linear optimization method solves the state estimation equations.

Reference [17] proposes estimation of voltage profile (and hence sag levels) along a distribution feeder using a limited measured points, based on radial connection characteristic and fault association in sags. Then, it employs a least-square method to predict the sag profile along a distribution line to calculate the feeder power quality indices such as the system Average RMS Frequency Index (SARFIx). The next contribution in this area optimizes the number and location of the meters for monitoring a large transmission network in terms of voltage sags, then deploys it for calculating voltage sag system indices [18].

C. Transient State Estimation (TSE)

TSE is a reverse function to transient simulation. While transient simulation is used to analyze the consequences of a disturbance on a power system voltage, current, etc., TSE is exploited to identify the cause of transient change in system parameters. Therefore, TSE can be used potentially as a valuable tool for diagnostic purposes in power systems.

Transient variations in TSE necessitate a time-domain solution for the system as well as a dynamic formulation to represent system components. The two broad classes of methods used in the digital simulation of the differential equations representing continuous systems are numerical solution of differential equations and difference equations, which are used by state variable formulation and Dommel's EMTP method [19], respectively.

Kent Yu [20]–[22] made a good contribution in this area by introducing the concept and the task of TSE to identify the cause of a transient change in voltages and currents of system by partial measurements. He used state variable formulation for modeling the system components to develop the measurement equation. However, one contribution [7] showed the possibility of using numerical integrator substitution (NIS), also known as Dommel's method, on a simple single-phase system with lumped components. The NIS approach has many advantages over the state variable formulation. Taking TSE further, this paper presents a three-phase formulation for TSE using NIS and its application. At present a three-phase transmission line model consisting of lumped PI sections, which allows representation of mutual coupling and unbalance has been implemented. Therefore this is more suitable for distribution systems where the line lengths are smaller than transmission. Even so multiple PI sections will need to be cascaded to represent some transmission lines.

In this paper the emphasis is on the framework and applicability of this new power quality state estimation technique rather than the component models, which will be refined and become more accurate as time progresses.

III. TSE Using NIS

A. Dynamic Model of System

Dommel's EMTP approach [23] combines the method of characteristics for transmission lines and trapezoidal rule for discretisation of the system elements. This results in a Norton equivalent for each system component. Fig. 3(a) shows the fundamental electrical circuit lumped elements, connected between two nodes k and m. Applying trapezoidal rule to the differential equation for each of them, results in the given Norton equivalent circuit as illustrated in Fig. 3(b).

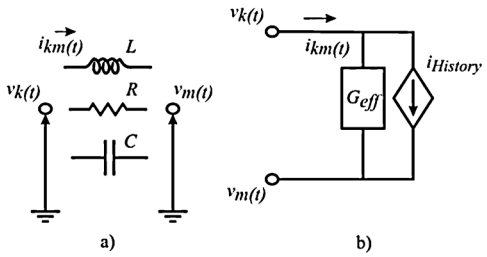

Fig. 3. (a) Basic electrical circuit elements. (b) Equivalent circuit diagram.

TABLE I
EQUIVALENT CIRCUIT DIAGRAM COMPONENTS

Element	INSTANTANEOUS TERM [G_{EFF}]	HISTORY TERM [$I_{HISTORY}$]
Resistor	$1/R$	-
Inductor	$\Delta t/2L$	$i_{km}(t-\Delta t) + G_{eff}\{v_k(t-\Delta t)-v_m(t-\Delta t)\}$
Capacitor	$2C/\Delta t$	$-i_{km}(t-\Delta t) - G_{eff}\{v_k(t-\Delta t)-v_m(t-\Delta t)\}$

Table I summarizes the conductance (instantaneous term) relating the current contribution to the voltage at the present time step (G_{eff}) and the current source (history term) which is the contribution to current from the previous time step quantities.

The power system can be described as a set of interconnected RLC branches. The relevant system components modeled in this paper are as follows (details can be found in [24]):

1) Transmission lines are modeled by three-phase PI model with coupled elements.
2) Transformers are modeled by three ideal single-phase transformer represented by a mutual inductance coupling between windings. Connection matrices are used to derive the nodal equation based on coil configuration (e.g., Delta/star-g, Star/star-g, etc.).
3) The real and reactive power components of the static loads are modeled by their equivalent resistance and inductance, respectively.

Considering voltages as state variables, the nodal solution is applied to form the entire network dynamic model. It leads to a coherent nodal system of equations to be solved as follows:

$$[G] \cdot \underline{v}(t) = \underline{i_s}(t) - \underline{I}_{\text{History}} \tag{1}$$

where $[G]$ is the conductance matrix, $v(t)$ is the vector of nodal voltages, $i_s\ (t)$ is the vector of external current sources and I_{History} is the vector current sources representing past history terms.

B. Transient State Estimator Formulation

The general form of the state estimation problem can be expressed as

$$\underline{z} = [H] \cdot \underline{x} + \underline{\varepsilon} \tag{2}$$

where z is an $(\text{m} \times 1)$ vector of measured quantities and x is an $(\text{n} \times 1)$ vector of state variables (unknown quantities) for which the equation must be solved. $[H]$ is an $(\text{m} \times \text{n})$ measurement function relating the known quantities to state variables and ε is the vector of measurement errors. For TSE, nodal voltages and branch and load currents are measured quantities and state variables are nodal voltages.

TABLE II
MEASUREMENT EQUATION CONSTRUCTION

Measurement Type	Measurement Vector Entry [z]	Measurement Matrix [H]	State Variables [x]
Nodal voltage to ground	$v_k(t)$	[1 0]	$[v_k(t) \ldots v_m(t)]^T$
Voltage across element	$v_k(t) - v_m(t)$	[1 -1]	
Branch current	$i_{km}(t)$-$I_{History}$	[G_{eff} -G_{eff}]	

With the growing concern regarding power quality, utilities have been installing PQ monitors that give voltage and current measurements and transmit this information to a central location. This information can be used as input for transient state estimator.

Each measurement point results in one equation that adds a corresponding row from the dynamic model into the measurement matrix, to form the transient state estimation problem. Table II illustrates how relevant entries must be selected for the fundamental electrical circuit elements shown in Fig. 3 and the relevant values defined in Table I.

C. TSE Solution and Observability

Once the state estimation problem is formed, it is solved for the state variables (nodal voltages). Singular value decomposition (SVD) is the selected approach in this paper.

The SVD factors the measurement matrix [H], which is $m \times n$, as a product of three matrices [26]:

$$[H] = [U] \cdot [W] \cdot [V]^T \tag{3}$$

where [U] and $[\text{V}]^{\text{T}}$ are orthogonal matrices and [W] is a diagonal matrix containing the singular values of H, hence $[\text{W}] = [diag(w_j)]$. The pseudo-inverse of the measurement matrix is

$$[H]^{-1} = [V] \cdot [W]^{-1} \cdot [U]^T. \tag{4}$$

If some of the w_j *values* $(j = 1, 2, \ldots, n)$ are zero or near zero, then the measurement matrix is singular. In this case, a zero is placed in the diagonal element of $[\text{W}]^{-1}$ [instead of $(1/w_j)$]. Then (5) is used to calculate state variables (nodal voltages):

$$\underline{x} = [V] \cdot [W]^{-1} \cdot [U]^T \cdot z. \tag{5}$$

The system is classified as over-determined, determined or under-determined, depending of the rank of $[H]$. Hence observability is determined by the number, position and type of measurements and also transformer winding configuration also greatly influences observability, as shown in [27].

TSE is normally an under-determined system due to the cost of measurement and results in some busbars being observable and others unobservable. In this case, SVD produces an infinite number of solutions that satisfies (2), expressed by

$$\underline{x} = \underline{x}_p + \sum_{i=0}^{N} (k_i \underline{x}_{ni}) \tag{6}$$

where $[x_p]$ is a particular solution, k_i is an arbitrary constant and $[x_{ni}]$ is the ith null-space vector. Hence any null-space can be added to $[x_p]$ and give another valid solution. The number of null-space vectors (N) is the number of zero w_j values in [W]. For observability the columns of [V] that form the null-space vectors are inspected and if all the ith entries are zero then adding any combination of the null-space vectors to particular solution will not change the value for the ith state variable (nodal voltage) and hence observable. Hence SVD provides observability analysis (OA) as a by-product by means of inspecting the null-space. Details and examples of this are given in [25] and [26].

D. TSE Implementation Summary

Fig. 4 summarizes the implementation of the proposed transient state estimator and the included blocks are described step by step as follows.

Step 1) The equations representing the dynamics of each system component, such as transformers, transmission lines, etc., are developed in form suitable for inclusion in (1).

Step 2) Individual equations combined to form dynamic model.

Step 3) Selection of measurement type and location.

Step 4) The corresponding rows of conductance matrix $[G_{\text{eff}}]$ constructed in step 2 are used to create the measurement equation $[H]$. For example in the case of instantaneous nodal voltage (v_k) measurement, the following entries are added to (2) (see Table II for more):

$$z_r(t) = v_k(t)$$
$$H_{r,k} = 1.0.$$

Step 5) If it is the first step $(t = 1)$ then initial current and voltages are set. Although power-flow results could be used for initialization in this work they are set to zero and TSE quickly settles in and tracks the system.

Step 6) The history terms are calculated and the measurement equation solved for the node voltages $(\underline{x})$.

Step 7) From the node voltages, the dependent variables such as branch currents are calculated.

Step 8) The calculated voltages and currents are used to update the history terms for the next time-step. The time-step (Δt) is 50 μs in this paper.

Step 9) The new measurement samples are used in (2) and solved for the state vector $(\underline{x})$.

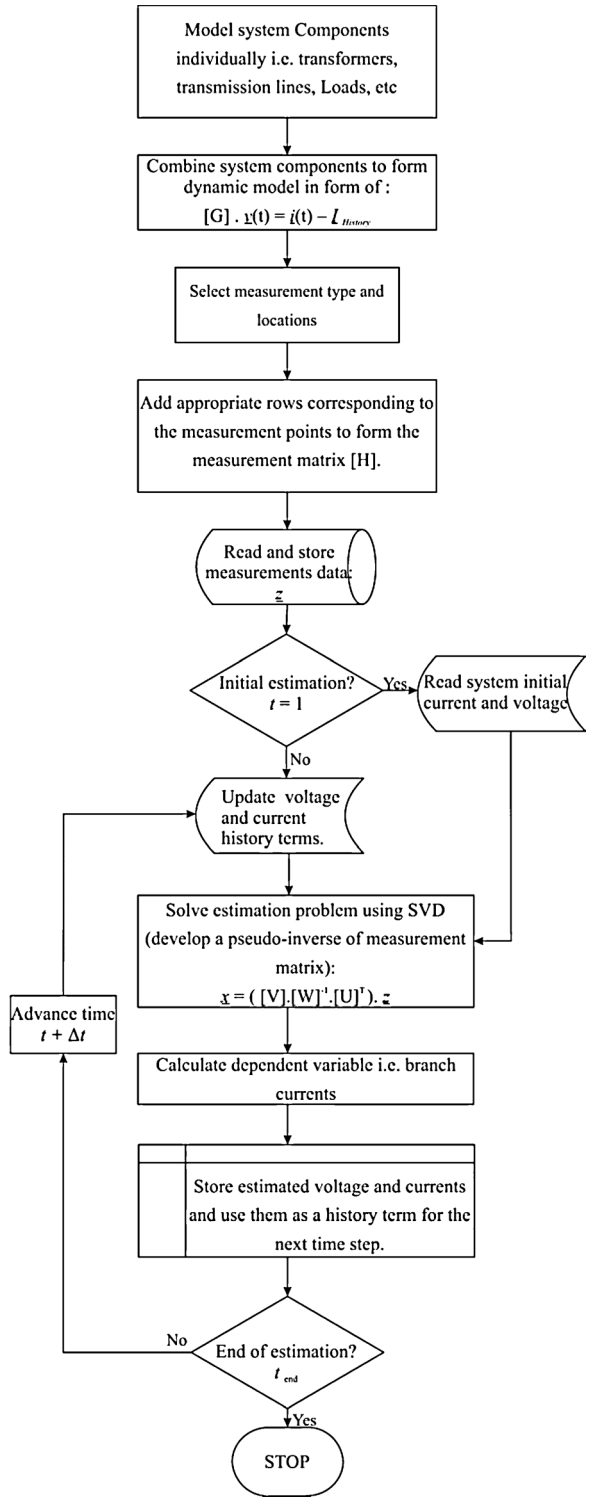

Fig. 4. Transient state estimator flowchart.

IV. Test System and Simulation Results

The test system is an 11-kV distribution network taken from Killinchy area, a rural area in south Canterbury, in the South Island of New Zealand. The system consists of a ring of 11-kV overhead lines and the lateral outgoing feeders. Symmetrical measurements are arbitrary placed at the points indicated on the network (see Fig. 5). The 11-kV grid is modeled as a Thevenin equivalent. Loads are represented by passive RL circuits.

Due to the lack of field measurements a PSCAD/EMTDC simulation is used to generate the field data (hereafter called measured or actual values). A single-phase short circuit at busbar No. 5 is simulated where no measurements on or near this busbar is located. This simulation shows an approximately 70% retained voltage on phases A and C recorded at busbar 11. The results from the simulation at the measurement points indicated in Fig. 5 are then fed to the developed transient state estimator (TSE) and the estimated quantities at the unmonitored locations are compared to the actual values for these locations. This is to investigate the accuracy of implemented TSE and its ability to identify the cause of the observed voltage dip/sag.

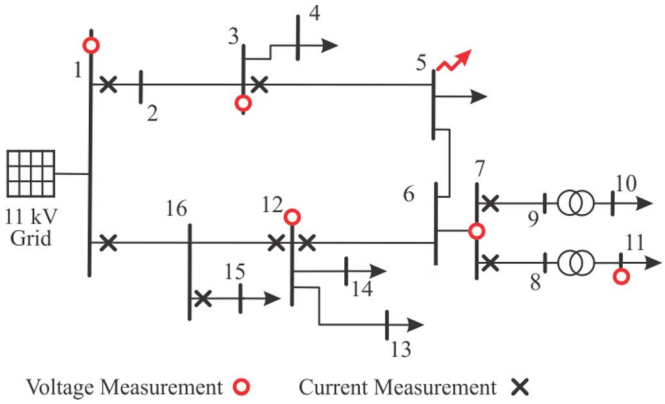

Fig. 5. Test system and measuring placement.

TABLE III
OBSERVABILITY CRITERIA

j	w_j	j	w_j	j	w_j	j	w_j
1	1.009992	**10**	1.000328	**19**	0.093641	**28**	0.017824
2	1.009992	**11**	1.000015	**20**	0.08464	**29**	0.010892
3	1.004738	**12**	1.000006	**21**	0.08464	**30**	0.010892
4	1.004738	**13**	1	**22**	0.045732	**31**	0.010328
5	1.002067	**14**	1	**23**	0.026324	**32**	0.010328
6	1.002067	**15**	1	**24**	0.025397	**33**	0.005316
7	1.000432	**16**	0.217903	**25**	0.025397	**34**	0.004737
8	1.00036	**17**	0.217903	**26**	0.0231	**35**	0.002729
9	1.000328	**18**	0.093641	**27**	0.0231	**36**	0.002161

It should be noted that the number of measurements are 39 (nodes) compared to 48 unknown state variables (nodes). It results in an under-determined estimation problem, hence observable and unobservable busbars are predicted. Using SVD only gives reliable answers for observable nodes. Observability is determined by the number, position and type of measurements and also transformer winding configuration also greatly influences observability as shown in [27].

Observability is illustrated by inspection of the relevant factor matrices ([W] and [V]). Table III shows the diagonal entries (w_j) of [W] which are not zero. The corresponding columns of V whose w_j's are equal to zero are shown in Table IV. The selected ith rows are correspond to unmonitored busbars 2, 4, 5 and 16 (nodes 4, 5, 6, 10, 11, 12, 13, 14, 15, 40, 41, 42). Inspecting the position of the zeros defines the observability. Busbar 5 (node 13, 14 and 15) is observable due to the fact that all corresponding entries for rows 13, 14 and 15 are zero, hence adding any combination of the null-space vectors to particular solution does not change the solution for this busbar. In contrast, busbar 4 is unobservable as adding the null-space vectors to the particular solution results in another solution for this busbar.

Fig. 6 illustrates a comparison between measured and estimated voltages at unmonitored nodes as a 3-D plot, to give an overview of the accuracy of the estimation of the whole system. It includes all nodes, both observable and unobservable. The unobservable nodes (10, 11 and 12 which are part of busbar 4 as a three-phase representation) are clearly evident by the error between the estimate and actual and the observability analysis indicates these nodes are not observable.

Fig. 7 depicts the estimation error for the observable nodes, before the fault inception, during the fault and after fault removal. The values are expressed as a percentage and are calculated according to (5):

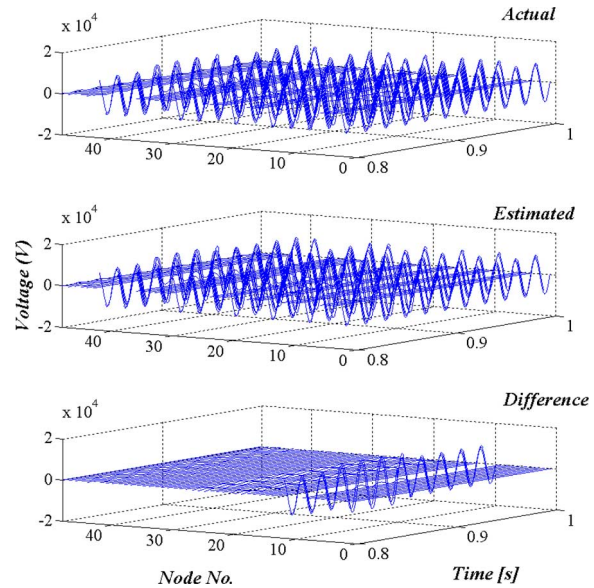

Fig. 6. Transient state estimation results.

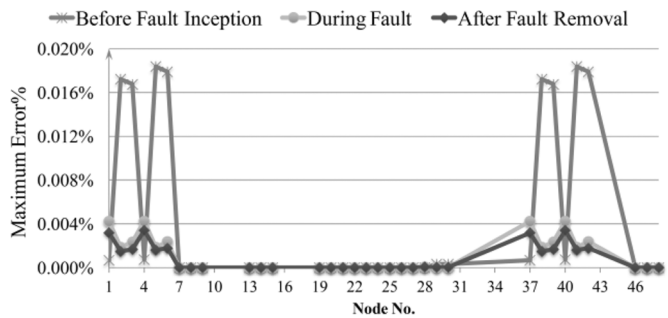

Fig. 7. Maximum percentage error in the voltage for the observable nodes (for the case shown in Fig. 6).

$$\text{Error\%} = 100 \times \left| \frac{v_{\text{actual}} - v_{\text{estimated}}}{\text{Maximum}(v_{\text{estimated}})} \right| \tag{7}$$

where *Maximum* $(v_{\text{estimated}})$ is the maximum estimated voltage for the healthy phases. *Maximum* $(v_{\text{estimated}})$ is used to normalize rather than $v_{\text{estimated}}$ to avoid divide by zero at zero-crossings. This shows that proposed TSE algorithm is accurate for observable busbars, even when the system is under-determined (number of measurements is less than the number of unknown state variables). However, as Smart Grids evolves the number of measurements is not likely to be the barrier it once was due to the massive amount of data that is becoming available.

Figs. 8–10 show the three-phase actual and estimated voltages at unmonitored busbars which are identified as observable busbars susceptible for the cause of recorded voltage dip/sag. For each busbar, the actual and estimated results are plotted as solid and dotted lines, respectively. However, they are indistinguishable due to the similarity. Inspection of the plotted voltages

TABLE IV
OBSERVABILITY CRITERIA

Node Number	37	38	39	40	41	42	43	44	45	46	47	48
4	0.0000	0.0000	0.0000	0.0000	0.0000	0.0000	0.0000	0.0000	0.0000	0.0000	0.0000	0.0000
5	0.0000	0.0000	0.0000	0.0000	0.0000	0.0000	0.0000	0.0000	0.0000	0.0000	0.0000	0.0000
6	0.0000	0.0000	0.0000	0.0000	0.0000	0.0000	0.0000	0.0000	0.0000	0.0000	0.0000	0.0000
10	-0.4075	-0.0379	0.4795	0.4072	0.4323	0.4249	0.0000	0.0000	0.0000	-0.1047	0.0598	-0.2344
11	-0.9132	0.0170	-0.2139	0.1817	-0.1929	-0.1896	0.0000	0.0000	0.0000	0.0467	-0.0266	0.1046
12	-0.0002	-0.8161	-0.2102	0.0088	0.0045	0.0608	0.0000	0.0000	0.0000	-0.0452	-0.4639	-0.2622
13	0.0000	0.0000	0.0000	0.0000	0.0000	0.0000	0.0000	0.0000	0.0000	0.0000	0.0000	0.0000
14	0.0000	0.0000	0.0000	0.0000	0.0000	0.0000	0.0000	0.0000	0.0000	0.0000	0.0000	0.0000
15	0.0000	0.0000	0.0000	0.0000	0.0000	0.0000	0.0000	0.0000	0.0000	0.0000	0.0000	0.0000
40	0.0000	0.0000	0.0000	0.0000	0.0000	0.0000	0.0000	0.0000	0.0000	0.0000	0.0000	0.0000
41	0.0000	0.0000	0.0000	0.0000	0.0000	0.0000	0.0000	0.0000	0.0000	0.0000	0.0000	0.0000
42	0.0000	0.0000	0.0000	0.0000	0.0000	0.0000	0.0000	0.0000	0.0000	0.0000	0.0000	0.0000

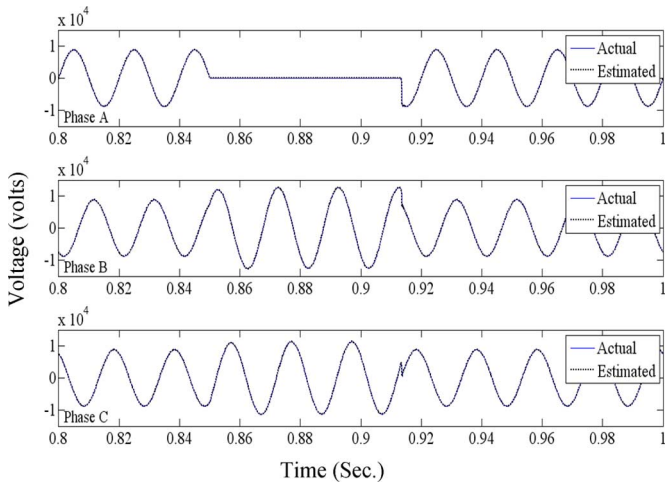

Fig. 8. Three-phase actual and estimated voltage at busbar No. 5.

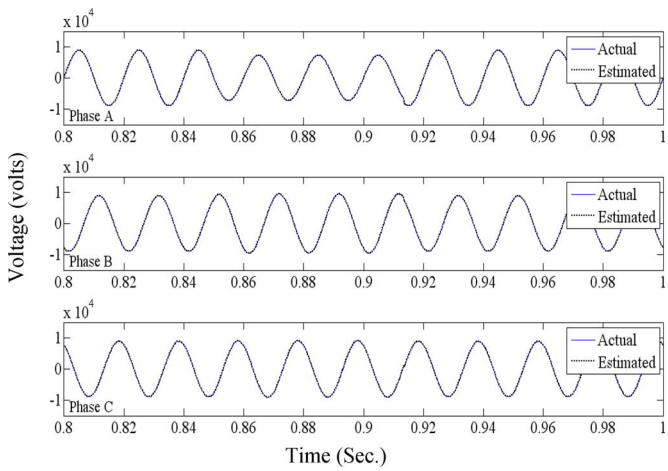

Fig. 9. Three-phase actual and estimated voltage at busbar No. 2.

verifies that a single-phase short circuit on phase A at busbar No. 5 occurred.

TSE With Measurement Noise: 5% Measurement noise (normally distributed at all measurement points) was added to the all measurement points and the TSE run once.

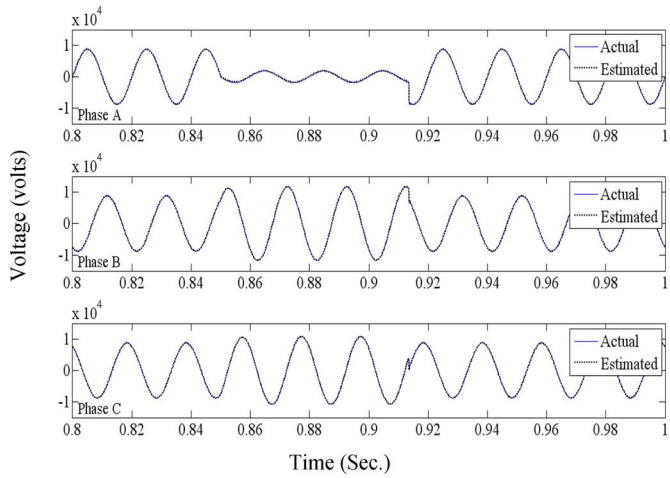

Fig. 10. Three-phase actual and estimated voltage at busbar No. 16.

Figs. 11 and 12 show the actual and estimated voltages and estimation error at busbar No. 5. Fig. 13 illustrates the maximum percentage voltage error at the identified faulted busbar, before the fault inception, during the fault and after fault removal. It clearly proofs that the developed TSE is able to make good estimates, even in the presence of measurement noise.

To show the robustness of the proposed TSE the following verifications have been performed using DIgSILENT's PowerFactory in order to reproduce more realistic conditions under which the TSE works. This time the simulated test system uses frequency dependent transmission line model with the frequency which the parameters of the lumped PI-models of the state estimator have been calculated. So the proposed TSE still uses the lumped PI-models while the actual measurements are taken from simulated network with frequency dependant line models (5% measurement noise is added). Different types of short circuits, including two phases with and without ground, as well as three-phase, have been simulated.

The new TSE was tested for its performance with different types of fault and the results are summarized in Table V. Due to space limitations, only the results for three unmonitored busbars, which were randomly selected, are shown. The percentage error was calculated according to (5) for the three

TABLE V
DIFFERENT TYPE OF FAULT AND PERCENTAGE ERROR

Busbar No.	Fault Type	Maximum Error (%) Before Fault Phase A	Before Fault Phase B	Before Fault Phase C	During Fault Phase A	During Fault Phase B	During Fault Phase C	After Fault Phase A	After Fault Phase B	After Fault Phase C
5	L-G	5.49%	5.44%	5.44%	11.78%	14.42%	14.37%	10.73%	13.70%	10.37%
	L-L	5.49%	5.44%	5.44%	7.40%	5.44%	10.31%	5.77%	5.44%	6.88%
	L-L-G	5.49%	5.44%	5.44%	11.61%	11.64%	13.20%	11.09%	14.07%	12.52%
	3-Ph-G	5.49%	5.44%	5.44%	10.55%	10.09%	10.06%	10.28%	16.36%	14.22%
6	L-G	8.86%	8.75%	8.75%	18.95%	24.35%	24.18%	12.37%	18.71%	15.11%
	L-L	8.86%	8.75%	8.75%	22.05%	8.75%	25.27%	8.83%	8.75%	10.21%
	L-L-G	8.86%	8.75%	8.75%	25.72%	16.59%	21.58%	12.38%	19.13%	15.12%
	3-Ph-G	8.86%	8.75%	8.75%	30.97%	14.26%	16.34%	14.58%	19.82%	18.11%
16	L-G	5.23%	5.16%	5.16%	5.15%	7.70%	7.77%	6.55%	7.67%	6.83%
	L-L	5.23%	5.16%	5.16%	6.89%	5.16%	6.10%	5.33%	5.16%	6.08%
	L-L-G	5.23%	5.16%	5.16%	5.15%	7.32%	9.00%	6.74%	8.04%	7.81%
	3-Ph-G	5.23%	5.16%	5.16%	5.15%	2.68%	2.49%	6.82%	9.91%	9.72%

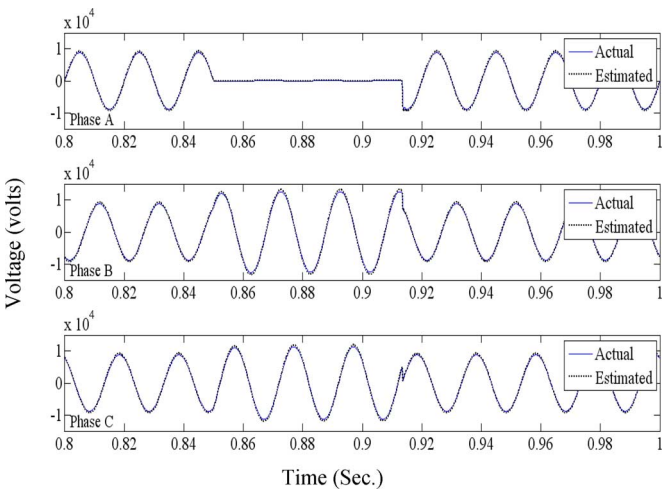

Fig. 11. Three-phase actual and estimated voltage at busbar No. 5 in presence of 5% measurement noise.

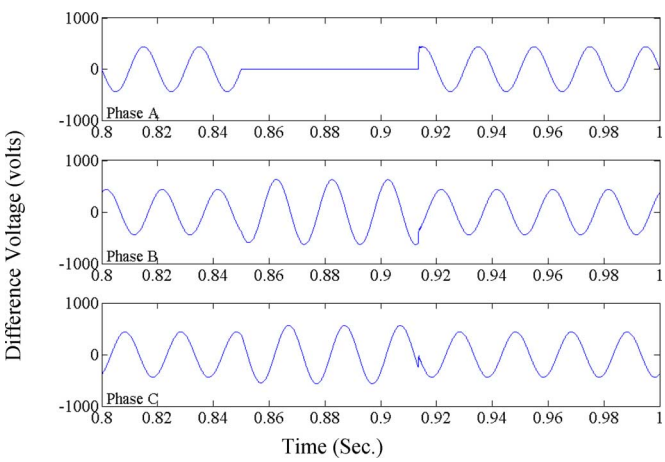

Fig. 12. Difference between measured and estimated voltages at busbar No. 5 in presence of 5% measurement noise.

periods (before fault inception, during the fault and after fault removal). Figs. 14–16 show the three-phase actual and estimated voltages at these observable busbars. The error values of

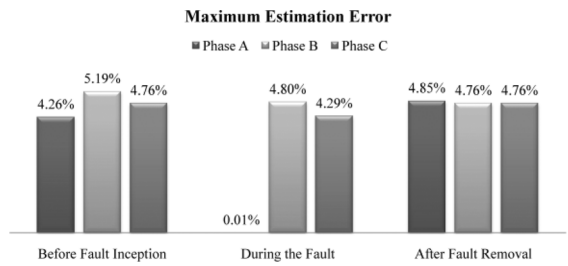

Fig. 13. Maximum voltage percentage error at busbar No. 5.

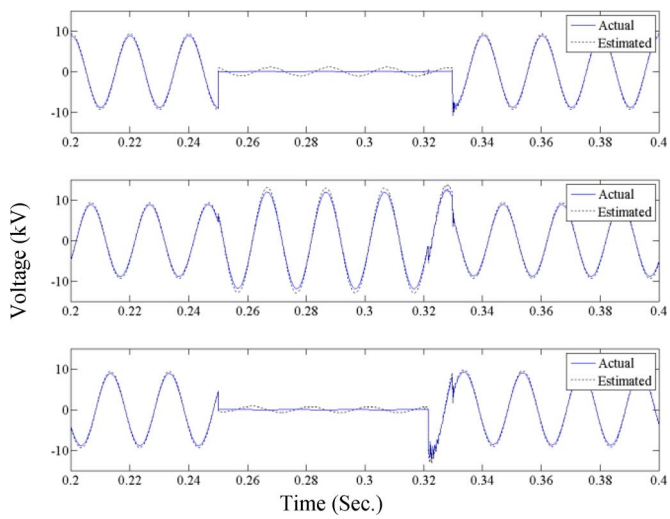

Fig. 14. Two-phase-to-ground short circuit actual and estimated voltage at busbar No. 5.

Table V are somewhat deceiving as the maximum error is one point and not indicative of the overall error at the other time points. For example the highest error, 30.97%, was on phase A at busbar 6 during the fault. Fig. 16 shows the comparison, which is good, with only one high error point and the rest typically have a maximum error of approximately 8%, This system is only partially observable moreover noise is included in the measurements which exasperate the estimation problem.

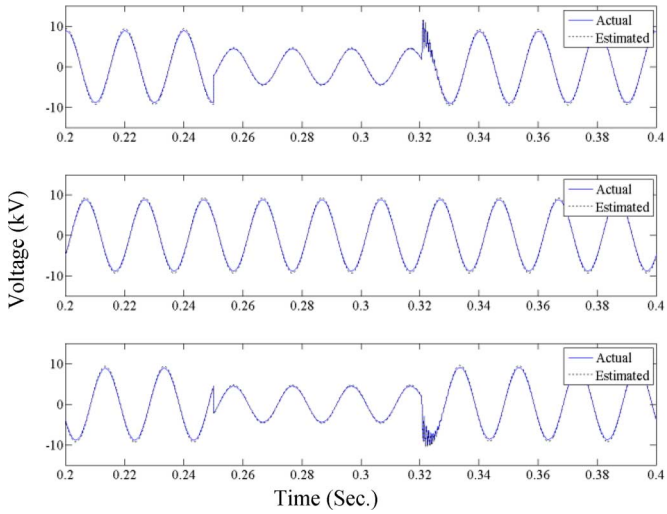

Fig. 15. Two-phase short circuit actual and estimated voltage at busbar No. 16.

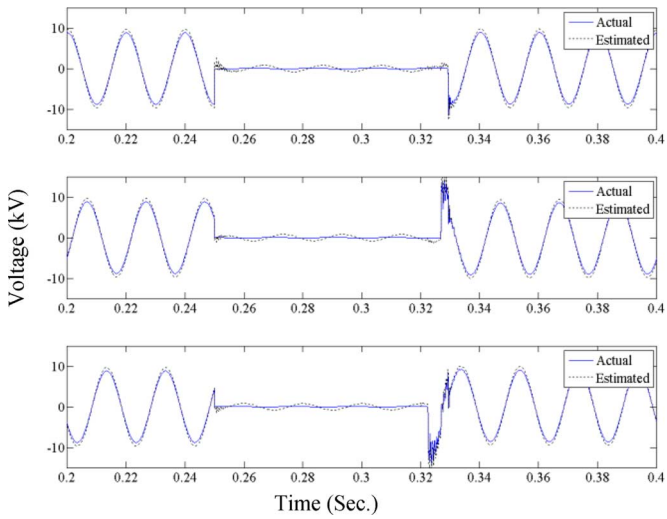

Fig. 16. Three-phase to ground short circuit actual and estimated voltage at busbar No. 6.

As can be seen the estimated results oscillate around the actual value during the fault period. This is mainly due to the difference in the transmission line representation (although other errors contribute slightly) and will be resolved if a travelling wave transmission line model was used in the TSE. As is the case for any transient study judicious selection of component models is needed to ensure fidelity of the results. A simplified representation is adequate for most of the components; however some components will have more of an influence on the waveforms at a given point and hence require more detailed modeling in order to faithfully reproduce the response at this point. This test case has shown the discrepancy expected when a simple transmission line model is used and the actual system is more complex (represented by a full travelling wave model). The results verify that proposed TSE algorithm is sufficiently accurate for identifying the location of disturbances as well as the voltages and currents at observable busbars and branches, even with a simple transmission line model. This was true for all the different types of faults tested even though the system is under-determined and measurement noise is included.

V. Conclusion

As the electrical network evolves into a Smart Grid new algorithms are needed to aid distribution system management. PQSE has been proposed as a smart algorithm for managing power quality issues in a smart grid environment where great amounts of data are available. The output from a PQSE can be used not only for detecting sources of power quality emissions but potentially also for taking remedial actions. The focus of this paper has been on one type of PQSE, transient state estimation.

A new three-phase TSE has been presented in this paper and its application to a realistic power system demonstrated. The implemented estimator has been applied to a partially observable test system and was successful in determining the voltage at observable busbars and currents in observable branches. One output from the TSE is the state variables that are observable. The results showed this is a promising technique as it is capable of identifying the source of recorded voltage dip/sag, even in the presence of 5% measurement noise in all measurement points.

The three-phase representation of the basic power system components has been developed and it has been demonstrated that TSE method based on NIS works and is sound. More work is needed to improve the models further. In particular incorporating travelling-wave transmission line model is important to increase the methods applicability to transmission systems.

References

[1] NIST Special Publication 1108, "NIST Framework and Roadmap for Smart Grid Interoperability Standards, Release 1.0," Jan. 2010.
[2] National Science And Technology Council, "A policy framework for the 21st century grid: Enabling our secure energy future," Jun. 2011.
[3] Transpower New Zealand Ltd., "Wairakei ring investment proposal, attachment E—Final long-list and short-list criteria," Dec. 2008.
[4] Transpower New Zealand Ltd., "Grid upgrade plan 2009, installment 6 part IX: Bunnythorpe-haywards thermal upgrade (2006) investment proposal," Jul. 2010.
[5] Transpower New Zealand Ltd., "Connecting and dispatching new generation in New Zealand: Overview," Jun. 2007.
[6] David Strong & Associates, "Development and implementation of system protection schemes," Electricity Commission, Jun. 2009.
[7] N. R. Watson, "Power quality state estimation," *Eur. Trans. Elect. Power*, vol. 20, pp. 19–33, Jan. 2010.
[8] G. T. Heydt, *Electric Power Quality*, 2nd ed. West Lafayette, IN, USA: Stars in a Circle Publications, 1991.
[9] G. T. Heydt, "Identification of harmonic sources by a state estimation technique," *IEEE Trans. Power Del.*, vol. 4, pp. 569–576, 1989.
[10] A. P. S. Meliopoulos *et al.*, "Power system harmonic state estimation," *IEEE Trans. Power Del.*, vol. 9, pp. 1701–1709, 1994.
[11] C. Madtharad *et al.*, "An optimal measurement placement method for power system harmonic state estimation," *IEEE Trans. Power Del.*, vol. 20, pp. 1514–1521, 2005.
[12] K. K. C. Yu and N. R. Watson, "Error analysis in static harmonic state estimation: A statistical approach," *IEEE Trans. Power Del.*, vol. 20, pp. 1045–1050, 2005.
[13] H. M. Beides and G. T. Heydt, "Dynamic state estimation of power system harmonics using Kalman filter methodology," *IEEE Trans. Power Del.*, vol. 6, pp. 1663–1670, 1991.
[14] Z. P. Du *et al.*, "Identification of harmonic sources of power systems using state estimation," *Proc. Inst. Elect. Eng., Gen., Transm. Distrib.*, vol. 146, pp. 7–12, 1999.
[15] N. Kanao *et al.*, "Power system harmonic analysis using state-estimation method for Japanese field data," *IEEE Trans. Power Del.*, vol. 20, pp. 970–977, 2005.
[16] E. Espinosa-Juarez and A. Hernandez, "A method for voltage sag state estimation in power systems," *IEEE Trans. Power Del.*, vol. 22, pp. 2517–2526, 2007.
[17] W. Bin *et al.*, "Voltage sag state estimation for power distribution systems," *IEEE Trans. Power Syst.*, vol. 20, pp. 806–812, 2005.

[18] G. Olguin *et al.*, "An optimal monitoring program for obtaining voltage sag system indexes," *IEEE Trans. Power Syst.*, vol. 21, pp. 378–384, 2006.
[19] N. R. Watson and J. Arrillaga, *Power Systems Electromagnetic Transients Simulation*. London, U.K.: Institution of Electrical Engineers, 2002.
[20] K. K. C. Yu and N. R. Watson, "Identification of fault locations using transient state estimation," in *Proc. Int. Power System Transient (IPST2005)*, Montreal, QC, Canada, 2005.
[21] K. K. C. Yu and N. R. Watson, "An approximate method for transient state estimation," *IEEE Trans. Power Del.*, vol. 22, no. 3, pp. 1680–1687, Jul. 2007.
[22] N. R. Watson and K. K. C. Yu, "Transient state estimation," in *Proc. 13th Int. Conf. Harmonics and Quality of Power (ICHQP)*, 2008, pp. 1–6.
[23] H. W. Dommel, "Digital computer solution of electromagnetic transients in single- and multiphase networks," *IEEE Trans. Power App. Syst.*, vol. PAS-88, pp. 388–399, 1969.
[24] H. W. Dommel, *Electromagnetic Transients Program Reference Manual (EMTP Theory Book)*. Portland, OR, USA: Bonneville Power Administration, 1986.
[25] J. Arrillaga *et al., Power System Quality Assessment*. New York, NY, USA: Wiley, 2000.
[26] W. H. Press, *Numerical Recipes: The Art of Scientific Computing*, 3rd ed. Cambridge, U.K.: Cambridge Univ. Press, 2007.
[27] K. K. C. Yu and N. R. Watson, "Three-phase harmonic state estimation using SVD for partially observable systems," in *Proc. 2004 Int. Conf. Power System Technology (PowerCon 2004)*, vol. 1, pp. 29–34.

Ali Farzanehrafat (S'12) was born in Tehran, Iran, where he received the B.Sc. and M.Sc. degrees in power engineering in 2004 and 2007, respectively. Currently, he is pursuing Ph.D. degree at the Electrical and Computer Engineering Department, University of Canterbury, Christchurch, New Zealand.

He worked in industries for 6 years. His area of research is power quality state estimation.

Neville R. Watson (SM'99) received the B.E. (Hons.) and Ph.D. degrees in electrical and electronic engineering from the University of Canterbury, Christchurch, New Zealand, in 1984 and 1988, respectively.

He is a Professor at the University of Canterbury. His main research area is computer simulation and analysis applied to power quality issues, in particular, harmonics, voltage fluctuations and electromagnetic transients. He has a special interest in modeling nonlinear loads and their interactions, from CFLs to HVDC schemes and aluminium smelters. More recently VSDs have been the focus of his work.